



American Journal of Applied Sciences 5 (2): 83-88, 2008
ISSN 1546-9239
© 2008 Science Publications

Tactile Distinction of an Artery and a Tumor in a Soft Tissue by Finite Element Method

¹Ali Abouei Mehrizi, ¹Siamak Najarian, ²Majid Moini, and
³Farhad Tabatabai Ghomshe

¹Artificila Tactile Sensing and Robotic Surgery Lab, Department of Biomechanics, Faculty of Biomedical engineering, Amirkabir University of Technology, Tehran, Iran

²Tehran University of Medical Sciences, Tehran, Iran

³University of Social Welfare and Rehabilitation Sciences, Tehran, Iran

Abstract: Tactile detection of a tumor and an artery in a tissue and distinction of a healthy artery from a stenotic artery, using finite element method, are presented. Four 2D models of tissue have been created: tissue itself, tissue including a tumor (TIT), tissue including a healthy artery (TIHA), and tissue including a stenotic artery (TISA). After solving four models with similar boundary conditions and loadings, the 2D tactile mappings and stress graphs for upper nodes of models, which have key importance for transferring tactile data, were explored. Then, by comparing these results, if the stress values of nodes were constant and equal, tissue is unlikely to have any tumor or artery embedded. Otherwise, if the stress graph included a peak, the tissue had a tumor or an artery. Additionally, it was observed that the stress graph of tissue including an artery is time-dependent in comparison with the tissue including a tumor. Further, it was concluded that a stenotic artery had larger stress peak than a healthy artery.

Keywords: Modeling, Tactile Sensing, Soft Tissue, Tumor, Artery, Stenosis, FEM

INTRODUCTION

Minimally invasive surgery (MIS) is a kind of surgery in which two or three incisions with nearly 1 cm diameter or so are being created on external surface of the body. Then, tiny long surgery tools are entered through these incisions into the body and the surgeon does the operation by these tools. Because of the numerous advantages of MIS, comparing with traditional open surgery, the researchers are putting a great deal of effort on optimizing the design and capabilities of its related tools. Some of these advantages are: reducing damage to healthy tissue, decreasing trauma, patients heal more quickly, reducing recovery times, etc.^[1, 2, 3]. MIS is now being widely used as one of the most preferred choices for various types of operations^[4, 5].

Despite its advantages and growing popularity, MIS suffers from one major drawback: it decreases the sensory perception of the surgeon and the surgeon might accidentally cut or incur damage to some of the tissues^[6, 7]. This effect is more pronounced when the surgeon approaches a target tissue while moving across other healthy tissues. This could happen during

grasping or manipulation of biological tissues such as veins, arteries, bones, etc.^[8, 9]. Any inhibitions on the surgeon's sensory abilities might lead to undesirable results^[10, 11, 12, 13]. One of the main difficulties encountered in this area is the inability in detecting the arteries embedded in tissues. Therefore, in laparoscopic surgeries like bringing the gall bladder out of body, the location of cutting is burnt for bloodshed prevention or some grippers are placed in each side of the cutting location^[14].

Although this subject is new, but many studies have been performed about detection of arteries in tissues and their stenosis. Nearly all of these studies have used imaging and ultrasound techniques^[15]. Beside their advantages, they also have some limitations including: a) vessels deep in the body are harder to see than superficial vessels, b) smaller vessels are more difficult to image and evaluate than larger vessels, c) calcification that occurs as a result of atherosclerosis may obstruct the ultrasound beam, and d) sometimes ultrasound cannot differentiate between a blood vessel that is closed and the one that is very nearly closed, because the weak volume of blood flow produces a weak signal. Therefore, a practical method

Corresponding Author: Prof. Siamak Najarian, No. 424, Hafez Avenue, Department of Biomechanics, Faculty of Biomedical Engineering, Amirkabir University of Technology, Tehran, Iran, P.O. Box 15875-4413. Tel: (+98-21)-6454-2378. Fax: (+98-21)-6646-8186

which could eliminate these limitations during the surgery process sounds very necessary. Artificial tactile sensing is a new technique for detecting of arteries in soft tissues by palpation^[16].

Unlike tumor detection, a very rare number of studies could be found in literature on detecting of an artery and the location of its stenosis by tactile method^[17, 18, 19, 20]. In one of studies related to tactile detection of arteries, a sensorized finger was constructed which was capable of detecting pulse rate and waveform at wrist artery and sensing bard nodules in a mock breast^[21]. It is noticeable that in this study, numerical solutions were not performed. In another study, a long 10 mm diameter probe was constructed with an array of tactile sensor set in the end of it^[22]. This sensor was pressed against the tissue of interest and pressure distribution was read out as electrical signal across contact area. Then, this information was processed and the presence of an artery in tissue was concluded. In this study, just like the pervious works, numerical solutions were not employed. The last study on artery detection is related to construction of a tactile sensor that can track a vessel with various curves in artificial tissue with silicon type by a programmable robot^[23]. Similar to pervious works, in this study, numerical solutions were not performed again.

In this paper; for the first time, we have investigated the detection of an artery and a tumor in a tissue and separation of these two categories from each other by using finite element method. Furthermore, we have modeled a 25% stenotic artery in a tissue and investigated the possibility of distinction of a healthy artery from a stenotic artery and presented a criterion in this regard.

MATERIALS AND METHODS

New minimally invasive surgical techniques prevent surgeon from directly touching and palpating internal tissue. Therefore, surgeon cannot be aware of the condition of internal tissue. For example, hard lumps in soft organs are detected by probing the tissue with the fingers; arteries are localized during dissection by feeling for a time varying pressure; or the structural integrity of a blood vessel wall is assessed by rolling it between the fingers.

In this paper, we scrutinized on presence of artery in soft biological tissue and distinction of a tumor to pattern out palpation by finite element method. We were also able to separate a healthy artery from a stenotic artery by simulating palpation.

In every application of tactile sensing method, the physical contact between tactile sensor and object or tissue is of special importance. In this physical contact, according to the design of sensor, a parameter of touch

was used as a criterion for stimulating a sensor. This criterion can be force, pressure (stress), displacement (strain), temperature, humidity, roughness, stiffness, and softness that is appeared on the surface of the touched object in which tactile data was transferred between it and the sensor. Otherwise, they cannot be a suitable criterion.

In the present study, we consider a phantom of soft tissue that includes an artery and a tumor as shown in Fig. 1. It has been divided into four parts: the tissue itself which is part *a*, tissue including a tumor (TIT) that is part *b*, tissue including a healthy artery (TIHA) that is part *c*, and tissue including a stenotic artery (TISA) which is part *d*. The cross section of each part, as shown in Fig. 2, has been selected as a 2D model. The cross section of model *b* and *c* pass through the center of tumor and stenotic artery, respectively. For modeling of palpation process by finger, a constant displacement (-7.5 mm) on top line of each model has been considered and Von Mises stress parameter was selected as a detection criterion in modeling. For completing the simulation of palpation effect, the bottom line of each model was constrained in *y*-direction as shown in Fig. 2.

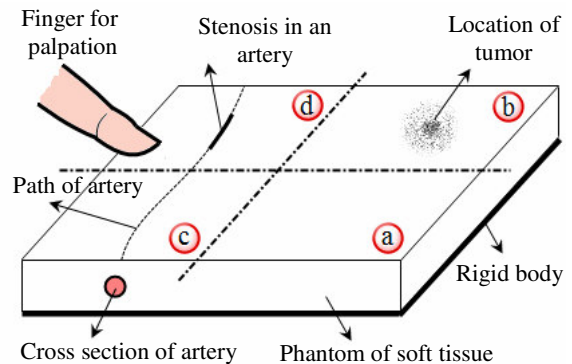


Fig. 1: Schematic representation of a soft tissue: *a*) the tissue itself, *b*) TIT, *c*) TIHA, and *d*) TISA.

As shown in Fig. 2, we considered four rectangles as four plane models of soft tissue, which each model had 80×30 mm dimension. In this modeling, two arteries and tumor were assumed completely circular and in center of tissue geometry. In model *b*, the diameter of tumor is 10 mm, in model *c* the wall thickness and internal diameter of artery are 8 mm and 1 mm, respectively, and in model *d* the stenosis thickness is 1 mm. Tissue, artery, and stenosis components were assumed elastic and isotropic material with a modulus of elasticity of 15, 300, and 600 kPa, respectively^[18, 24, 25]. The modulus of elasticity of tissue has been assumed 20 times larger than tissue^[18].

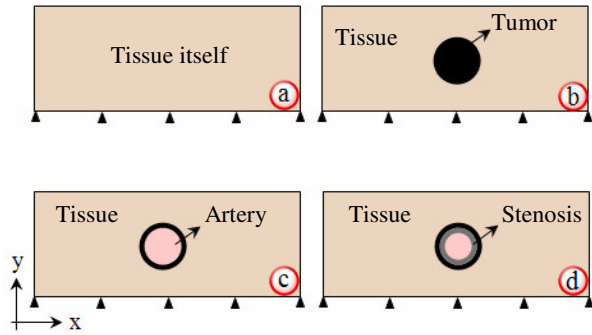


Fig. 2: The cross section of each part shown in Fig. 1.

In models *c* and *d*, blood fluid has been omitted but instead its effect on artery wall has been considered for duration of a healthy pulse, which is approximately 0.85 second. This effect has been applied as pressure loading with a maximum and a minimum of inside pressure of artery to be 120 and 80 mmHg, respectively. This loading has been divided into two steps: systolic and diastolic phases which loading time for each phase is 0.425 second. In systolic step, pressure increases from 80 to 120 mmHg as linear during the first 0.425 second and in diastolic step it decreases from 120 to 80 mmHg as linear during the next 0.425 second.

This model has been solved by finite element method. The length of each model has been considered 80 mm so that the left and right side tissues be far from artery and tumor and do not affect the stress distribution of artery, tumor and their environments. Bottom side of tissue in each model has been fixed in the *y*-direction that is the direction of loading on top side of model. With prevention of rigid body motion, each model was solved for a duration of 0.85 second. For having continuous strain in touch site of artery and tumor with tissue, they were glued to tissue by gluing same nodes together. Model has been meshed by a 4-node bilinear plane stress quadrilateral element.

To gain accurate solution and reduce the duration of solving process, element size of tumor, arteries, and the environments that have severe gradients of stress were considered finer than other parts of model.

The aim of this modeling is to explore the effect of an artery, a stenotic artery, and a tumor in tissue and their comparison with each other for finding a criterion for separating them. Therefore, Von Mises stress graph for all of nodes created in top side of four models, shown in Fig. 2, and 2D tactile image of models were explored.

RESULTS AND DISCUSSION

For every model, outputs in two different situations were derived: 1) stress distribution on top side of tissue model that is the site of touch between tissue and sensor. This was named 2D tactile image and 2) Von Mises stress graph on all of top nodes. According to 2D tactile imaging and stress graph, the results are as follows:

Appearance of the symptoms of existence of an artery or a tumor on top side of tissue model: this result supports the suitability of artificial tactile sensing method in artery or tumor detection and separation of a healthy artery, stenotic artery, and tumor from each other. Fig. 3 shows 2D tactile images corresponded by applying -7.5 mm displacement on top line of each model. From the 2D tactile images *b*, *c*, and *d*, it is understood that applied pressure on the tissue which has tumor or artery, caused a non-uniform stress distribution in comparison with the tissue itself.

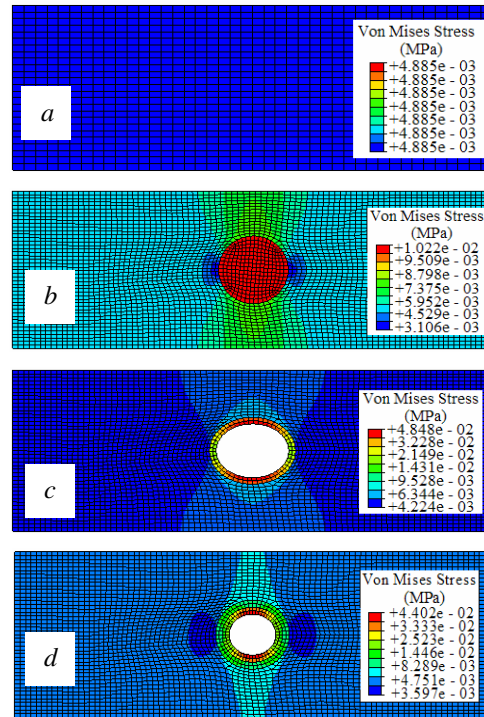


Fig. 3: 2D tactile image *a*) the tissue itself, *b*) TIT, *c*) TIHS, and *d*) TIAS (tactile images *c* and *d* are related to time 0.425 second that internal pressure of artery reaches 120 mmHg).

Appearance of a peak in stress graph: as shown in Figs. 4, 5, and 7, Von Mises stress graphs derived for

the nodes on top side of models *b*, *c*, and *d*, in comparison to model *a*, include a peak. The peak for these three graphs is a symptom for existence of tumor or artery in tissue. Also, the centers of peaks are exactly under tumor or artery. Therefore, we can determine the exact location of artery or tumor through stress graph. By comparing Figs. 6 and 7, it is clear that the derived result for model *b* has a good compliance with other studies^[20].

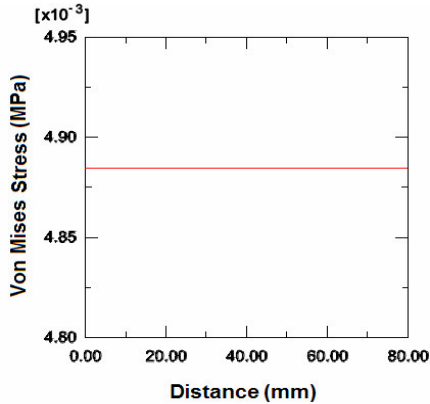


Fig. 4: Von Mises stress graph for nodes on top side of model *a* (this graph is the same during 0.85 second).

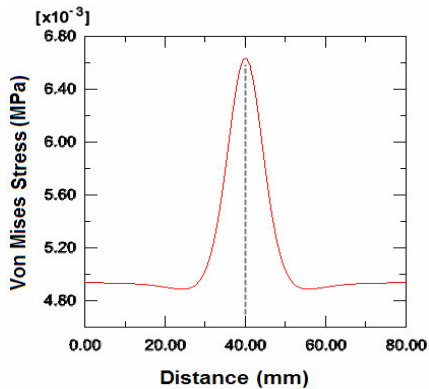


Fig. 5: Von Mises stress graph for nodes on top side of model *b* (this graph is the same during 0.85 second).

Since models *c* and *d* have a time-dependent loading inside artery wall, their stress graphs vary with time. In other words, the value of stress peak is time-dependent. This variation has been presented for initial time (0 second), end time (0.425 second) of systolic step, and two other times between initial and end time of this step in Table 1.

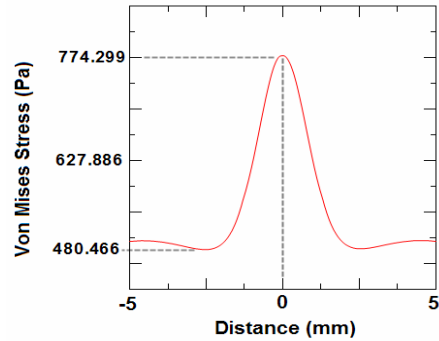


Fig. 6: Von Mises stress graph for nodes on top side of the model of tissue including a tumor^[20].

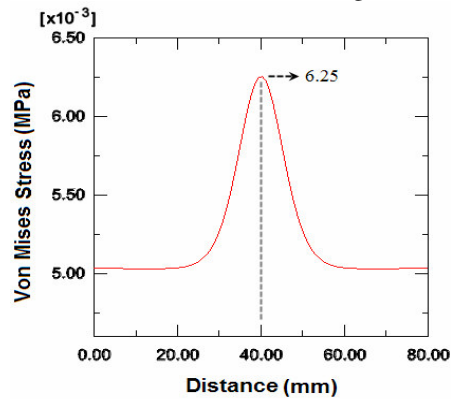


Fig. 7: Von Mises stress graph for nodes on top side of model *c* at 0.425 second of systolic step.

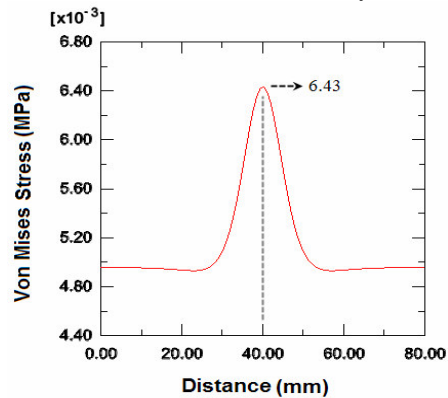


Fig. 8: Von Mises stress graph for nodes on top side of model *d* at 0.425 second of systolic step.

In Table 1, for model TIHA and TISA, the Von Mises stress has been presented for four times of systolic step. It is deduced that for TISA model, the variation range of Von Mises stress from 0 to 0.425 seconds in systolic step is smaller than TIHA model, but the value of its Von Mises stress is larger than TIHA model.

Table 1: The value of Von Mises stress for four times in systolic step for models TIHA and TISA

Model	Von Mises stress ($\times 10^{-3}$ MPa)			
	0.00 (s)	0.159 (s)	0.349 (s)	0.425 (s)
TIHA	5.550	5.740	6.102	6.254
TISA	6.281	6.322	6.400	6.432

Since pressure inside of artery increases as linear in systolic step from 80 to 120 mmHg and decreases as linear in diastolic step from 120 to 80 mmHg, we derive a graph similar to graphs shown in Figs. 7 and 8 for diastolic step.

In this study, the palpation of physician was modeled and simulated by finite element method. This modeling has been performed for four 2D tissue models: tissue itself, tissue including a tumor, tissue including an artery, and tissue including a stenotic artery.

By comparing 2D tactile images *a*, *b*, *c*, and *d* in Fig. 3, we can see that with applying the same loading on top side of each model shown in Fig. 2, 1) if 2D tactile image was uniform (Fig. 3-a) there is only the tissue itself, 2) if 2D tactile image was not uniform, the tissue includes other material with different mechanical properties of soft tissue like tumor or artery (Figs. 3-b, c, and d), 3) if 2D tactile image was not uniform but remained constant versus time, the tissue includes tumor (Fig. 3-b), 4) if 2D tactile image was neither uniform nor constant, the tissue includes artery (Figs. 3-c and d). With comparing Von Mises stress graphs shown in Figs. 4, 5, 7, and 8, we can conclude that with applying the same loading on top side of each model shown in Fig. 2, 1) if stress values versus top nodes and time be constant (Fig. 4) there exists the tissue itself, 2) if stress graph consists a peak, the tissue includes other material with different mechanical properties of soft tissue like tumor or artery (Figs. 5, 7, and 8), 3) if the value of stress peak versus time be constant, the tissue includes tumor (Fig. 7), 4) if the value of stress peak be time-dependent, the tissue includes artery (Figs. 7 and 8), and 5) if we compare the peaks of two time-dependent stress graphs at same time for a same and proper loading, the peak that has larger value belongs to the stenotic artery, because a stenotic artery divulges more strength than a healthy artery in the same conditions.

Therefore, based on the division presented in Table 2, we cannot separate a healthy artery of a stenotic artery only with comparing their 2D tactile image but we can distinct them from each other by comparing their stress graphs.

Table 2: The comparison of results for four models.

Model	2D tactile image	Von Mises stress graph
Tissue itself	Uniform and time-independent	A constant value and time-independent
TIT	Non uniform and time-independent	A peak and time-independent
TIHA and TISA	Non uniform and time-dependent	A peak and time-dependent

CONCLUSION

In this study, by creating four tactile models and exploring 2D tactile image and stress graphs for each one and comparing them together, we could detect the existence of a tumor or an artery in tissue. According to the obtained results, we were able to separate the tissue itself from tissue including a tumor, and tissue including an artery as presented in Table 2. A noticeable finding in this modeling is the distinction of a healthy artery from a stenotic artery by comparing the values of their Von Mises stress peak together as presented in Table 1.

ACKNOWLEDGEMENTS

The authors gratefully acknowledge the Faculty of Biomedical Engineering of Amirkabir University of Technology (Tehran Polytechnic), and the Center of Excellence in Biomedical Engineering of Iran, for their help in conducting this project.

REFERENCES

- Dario, P., 1991. Tactile Sensing-Technology and Applications. *Sensors and Actuators A-Physical*, 26(1/3): 251-261.
- Dargahi, J., S. Najarian, 2004. Analysis of a Membrane Type Polymeric-Based Tactile Sensor for Biomedical and Medical Robotic Applications. *Sensors and Materials*, 16(1): 25-41.
- Dargahi, J., S. Najarian, 2004. An Integrated Force-Position Tactile Sensor for Improving Diagnostic and Therapeutic Endoscopic Surgery. *Bio-Medical Materials and Engineering*, 14(2): 151-166.
- Dargahi, J., 1998. Piezoelectric and Pyroelectric Transient Signal Analysis for Detecting the Temperature of an Object for Robotic Tactile Sensing. *Sensor and Actuators A-Physical*, 71(1/2): 89-97.

5. Dargahi, J., S. Najarian, K. Najarian, 2005. Development and 3-Dimensional Modeling of a Biological Tissue Grasper Tool Equipped with a Tactile Sensor. accepted for publication in Canadian Journal of Electrical and Computer Engineering, 30(4): 225-230.
6. Brouwer, I., J. Ustin, L. Bentley, A. Sherman, N. Dhruv, F. Tendick, 2001. Measuring in vivo Animal Soft Tissue Properties for Haptic Modeling in Surgical Simulation. In Studies in Health Technology Informatics - Medicine Meets Virtual Reality, Amsterdam: ISO Press, 69-74.
7. Dargahi, J., S. Najarian, 2004. A Supported Membrane Type Sensor for Medical Tactile Mapping. Sensor Review, 24(3): 284-297.
8. Hannaford, B., J. Trujillo, M. Sinanan, M. Moreyra, J. Rosen, J. Brown, R. Leuschke, M. MacFarlane, 1998. Computerized Endoscopic Surgical Grasper. In Studies in Health Technology Informatics-Medicine Meets Virtual Reality, Amsterdam, ISO Press, 265-271.
9. Dario, P., M.C. Carrozza, L. Lencioni, B. Magnani, S. D'Attanasio, 1997. A Micro Robotic System for Colonoscopy. Proc. IEEE Int. Conf. on Robotics and Automation, IEEE Robotics and Automation Society, 1567-1572.
10. Dargahi, J., S. Najarian, 2004. Theoretical and Experimental Analysis of a Piezoelectric Tactile Sensor for Use in Endoscopic Surgery. Sensor Review, 24(1): 74-83.
11. Fischer, H., B. Neisius, R. Trapp, 1995. Interactive Technology and a New Paradigm for Health Care. IOS Press, The Netherlands.
12. Howe, R.D., W.J. Peine, D.A. Kontarinis, J.S. Son, 1994. Remote Palpation Technology. Proceedings of IEEE Engineering in Medicine and Biology Magazine, 14(3): 318-323.
13. Bicchi, A., G. Canepa, D.De. Rossi, P. Iacconi, E.P. Scilingo, 1996. A Sensorized Minimally Invasive Surgery Tool for Detecting Tissue Elastic Properties. Proceedings of IEEE International Conference Robotics and Automation, Minneapolis, USA, 884-888.
14. Dargahi, J., S. Najarian, 2004. Human Tactile Perception as a Standard for Artificial Tactile Sensing-a review. International Journal of Medical Robotics and Computer Assisted Surgery, 1(13): 23-35.
15. Dargahi, J., S. Najarian, 2005. Advances in Tactile Sensors Design/Manufacturing and Its Impact on Robotics Applications- a review. Industrial Robot, 32(3): 268-281.
16. Dargahi, J., S. Najarian, 2003. An Endoscopic Force Position Grasper with Minimum Sensors. Canadian Journal of Electrical and Computer Engineering, 28(3/4): 155-161.
17. Dargahi, J., S. Najarian, X.Z. Zheng, 2005. Measurements and Modeling of Compliance Using a Novel Multi-Sensor Endoscopic Grasper Device. Sensors and Materials, 17(1): 7-20.
18. Mirbagheri, A., J. Dargahi, S. Najarian, F. Tabatabai Ghomshe, 2007. Design, Fabrication, and Testing of a Membrane Piezoelectric Tactile Sensor with Four Sensing Elements, American Journal of Applied Sciences, 4(9): 645-652.
19. Hosseini, S.M., S. Najarian, S. Motaghinasab, Sh. Torabi, 2007. Experimental and numerical verification of artificial tactile sensing approach for predicting tumor existence in virtual soft tissue. Proceedings of the 15th Annual-International Conference of Mechanical Engineering, Amirkabir University of Technology, Tehran, Iran.
20. Hosseini, S.M., S. Najarian, S. Motaghinasab, J. Dargahi, 2006. Detection of Tumors Using Computational Tactile Sensing Approach. International Journal of Medical Robotics and Computer Assisted Surgery, 2(4): 333-340.
21. Dario, P., M. Bergamasco, 1988. An Advanced Robot System for Automated Diagnostic Tasks through Palpation. IEEE Transactions on Biomedical Engineering, 35(2): 118-26.
22. Peine, W.J., J.S. Son, R.D. Howe, 1994. A Palpation System for Artery Localization in Laparoscopic Surgery. First International Symposium on Medical Robotics and Computer-Assisted Surgery, Pittsburgh, 22-24.
23. Beasley, R.A., R.D. Howe, 2002. Tactile Tracking of Arteries in Robotic Surgery. Proceedings of the 2002 IEEE, International Conference on Robotics & Automation, Washington, DC.
24. Chandran, K., 1992. Cardiovascular Biomechanics. New York University Press.
25. Radj, A., L. Chris, A. Johannes, 2004. Finite element modeling and intravascular ultrasound elastography of vulnerable plaques: parameter variation. Ultrasonics, 42: 723-729.